MOLECULAR AND CELLULAR BIOLOGY, July 1986, p. 2298–2304
0270-7306/86/072298-07$02.00/0

Vol. 6, No. 7

A DNA Fragment Containing the Upstream Activator Sequence Determines Nucleosome Positioning of the Transcriptionally Repressed *PHO5* Gene of *Saccharomyces cerevisiae*

LAWRENCE W. BERGMAN

Department of Biological Sciences, University of Maryland Baltimore County, Catonsville, Maryland 21228

Received 8 January 1986/Accepted 1 April 1986

The functional relationship of nucleosome positioning and gene expression is not known. Using high-copy plasmids, containing the yeast phosphate-repressible acid phosphatase gene (*PHO5*) and the *TRP1/ARS1* vector system, I have determined the nucleosomal structure of the 5′ region of the *PHO5* gene and demonstrated that the nucleosomal positioning of this region is independent of orientation or position in the various plasmid constructions utilized. However, deletion of a 278-base pair *Bam*HI-*Cla*I fragment from the 5′-flanking sequences of the *PHO5* gene causes the nucleosome positioning to become dependent on orientation or position in the plasmids tested. Use of *PHO5-CYC1-lACZ* fusions have demonstrated that this DNA fragment contains the sequences responsible for the transcriptional regulation of the *PHO5* gene in response to the level of phosphate in the growth media. The nucleosome positioning in the 5′ region of *PHO5* may be determined by an interaction with the sequences or machinery responsible for transcriptional regulation of the gene.

Numerous studies have demonstrated that the sequences immediately upstream from transcribed genes have an altered chromatin structure. These regions have been shown to have enhanced accessibility to a wide variety of nucleases such as DNase I, micrococcal nucleases, and restriction endonucleases (14, 23). Despite this intense study, the molecular mechanisms which result in this enhanced accessibility remain largely unknown. Also, in several systems, the precise positioning (or "phasing") or nucleosomes has been described; however, the relationship between this nucleosomal alignment and gene expression is not known. The detailed structure and nucleoprotein composition of gene upstream regions are of extreme interest in that these regions contain sequences important in the control of gene expression and presumably are the sites for interaction of *trans*-acting transcriptional regulatory factors. The chromatin structure of this region may contribute significantly to the control of gene expression.

The phosphate-repressible acid phosphatase gene system presents an attractive model to investigate the structural components and structural changes associated with the transition from a repressed state to a fully derepressed or transcriptionally active state. Previous studies by Bostian and co-workers have demonstrated that the acid phosphatase gene, encoded by the *PHO5* locus, is transcriptionally regulated in response to the level of phosphate on the growth media (17); i.e., in low-phosphate media, the gene is actively expressed, whereas in high-phosphate media the gene is fully repressed. Also, Oshima and co-workers have isolated a number of unlinked mutations which affect the regulation of acid phosphatase expression (22). Recent evidence has suggested that the *trans*-acting regulatory factors are expressed constitutively (9, 22). Furthermore, a model for the regulation of *PHO5* expression has been proposed (22). These findings present distinct advantages for the system in an investigation of chromatin structure.

In this study, I have utilized the finding that *PHO5* sequences present on multicopy plasmids appear to be transcriptionally regulated in a normal manner (2, 9) to analyze the nucleosomal structure of the 5′-upstream sequences of the transcriptional repressed *PHO5* gene.

MATERIALS AND METHODS

Yeast strains, bacterial strains, and media. Strains of *Saccharomyces cerevisiae* utilized in this study are listed in Table 1. Strains were grown in YCAD (6.7 g of yeast nitrogen base, 5.0 g of Casamino Acids, 0.4 g of adenine, and 20 g of glucose per liter supplemented with 20 μg of uracil or tryptophan per ml) or low-phosphate YCAD prepared according to Rubin (18). Bacteria were grown and plasmid DNA was isolated as described previously (13).

Plasmid construction. The construction of the 3.4-kilobase (kb) *PHO5/TRP1/ARS1* plasmid was described previously (2). Also, the 1.9-kb *Bam*HI-*Pst*I fragment was cloned into the multicloning site linker of pUC18, termed p19 (25). Subsequently, the 2.1-kb *Eco*RI-*Bam*HI fragment which lies immediately upstream of the *PHO5* gene was cloned into the appropriate sites of p19, to construct p1921. In each case (p19 and p1921), the 1.45-kb *TRP1/ARS1 Eco*RI fragment was cloned into the unique *Eco*RI site of each plasmid in both orientations. These plasmids were used to transform strain GG100-140 (Table 1).

The 278-base pair (bp) *Bam*HI-*Cla*I fragment was deleted from each *PHO5/TRP1/ARS1* plasmid by digestion with *Bam*HI and *Cla*I and conversion to a blunt-ended fragment, using the large fragment of DNA polymerase I; subsequently it was ligated with T4 DNA ligase. (The deletion in YAP106 was constructed in a similar manner except the individual digestion was done with *Xho*II and *Cla*I.)

The *PHO5-CYC1-lacZ* plasmids were constructed by the addition of *Xho*I linkers to the 278-bp *Bam*HI-*Cla*I. The resulting fragment was cloned in both orientations into a derivative of pLG669Z (6) (obtained from L. Guarente) which lacks the 430-bp *Xho*I fragment containing the regulatory sequences of the *CYC1* gene. The resulting plasmids, termed pZ278A and pZ278B, were used to transform the strains listed in Table 1. pE602B is a *PHO5-lacZ* protein fusion obtained from K. Bostian.

TABLE 1. Genotype and phenotype of *S. cerevisiae* strains utilized in this study

Strain	Genotype	Phenotype
JL6B	a *ura3-52 trp1 leu2-3 leu2-112 cry1*^{r}	Wild type
GG100-14D	a *pho5 his3 ura3-52 trp1*	Recessive nonderepressible
YAT29-40	a *pho80 ura3-52 trp1 leu2-3 leu2-112 ade2*	Recessive constitutive
YAT42-6B2	a *pho4 trp1 ura3-52 leu2-3 leu2-112*	Recessive nonderepressible
YAT41-3A	a *pho2 ura3-52 trp1 arg6*	Recessive nonderepressible
YAT242-2A	a *pho81 trp1 leu2-3 leu2-112*	Recessive nonderepressible

Preparation of minichromosome and nuclease digestion. The plasmid-containing fraction was prepared essentially as described previously except the spheroplasts were lysed in a buffer containing 25 mM Tris (pH 8.0)–100 mM NaCl–2 mM $MgCl_2$–1 mM $CaCl_2$–10 mM sodium butyrate–0.5% Triton X-100–1 mM phenylmethylsulfonyl fluoride. The samples were digested with 20 U of micrococcal nuclease per ml for various times at 37°C. To analyze the sequence preference of micrococcal nuclease on protein-free DNA, the plasmid-containing fraction was extracted with phenol, precipitated with ethanol, suspended in the original volume of lysis buffer, and digested with 20 U of micrococcal nuclease per ml for short intervals at 37°C. Reactions were terminated by addition of an equal volume of 20 mM EDTA–2% sodium dodecyl sulfate, subsequently extracted with phenol, phenol-chloroform (1:1), and chloroform, and precipitated with 2.5 volumes. The precipitates were suspended and digested with various restriction enzymes according to the specifications of the supplier.

Preparation of ^{32}P-labeled DNA hybridization probes. All hybridization probes described in the text were prepared by polyacrylamide gel electrophoretic purification of plasmid DNA digested with the appropriate restriction enzymes. The fragments were labeled by a fill-in reaction with ^{32}P-labeled deoxynucleotides and the large fragment of DNA polymerase I.

Gel electrophoresis and hybridization. Analysis of micrococcal nuclease-digested DNA was done on 1.2% agarose gels in a buffer system containing 20 mM Tris (pH 7.9)–2 mM sodium acetate–2 mM EDTA. Transfer of DNA from the agarose gel to nitrocellulose was performed essentially as described by Southern (20). Hybridization with ^{32}P-labeled DNA probes was carried out in 5× SSPE (1× SSPE is 180 mM NaCl, 10 mM sodium phosphate phosphatase [pH 7.0], 1 mM EDTA)–0.5% sodium dodecyl sulfate–5× Denhardt solution–1 mg of denatured salmon sperm DNA per ml for 16 to 24 h at 70°C. The filters were washed in 0.1× SSPE–0.1% sodium dodecyl sulfate at 70°C, dried, and subjected to autoradiography. The autoradiographs were scanned with a Joyce-Loebl densitometer with molecular weight standardization, using a mixture of gel-purified fragments prepared from *TRP1/ARS1* DNA (601-bp *Eco*RI-*Bgl*II fragment or 615-bp *Eco*RI-*Hin*dIII fragment, 838-bp *Hin*dIII-*Eco*RI fragment or 852-bp *Bgl*II-*Eco*RI fragment, 1,267-bp *Xba*I-*Eco*RI fragment, 1,453-bp *Eco*RI fragment).

Measurement of β-galactosidase and acid phosphatase. Cells were collected for β-galactosidase measurement by centrifugation and suspended in 0.1 volume of cold extraction buffer. Cell extracts were prepared by breakage with glass beads and assays were performed as described by Miller (15). The activity was normalized to the protein concentration of the extract, which was measured by the dye-binding method of Bradford (Bio-Rad Laboratories) with bovine serum albumin as the standard. β-Galactosidase activity is expressed as nanomoles of *O*-nitrophenyl-β-D-galactoside cleaved per minute per milligram of protein.

Acid phosphatase was measured directly in whole-cell suspensions by a spectrophotometric assay, using 2.25 mg of

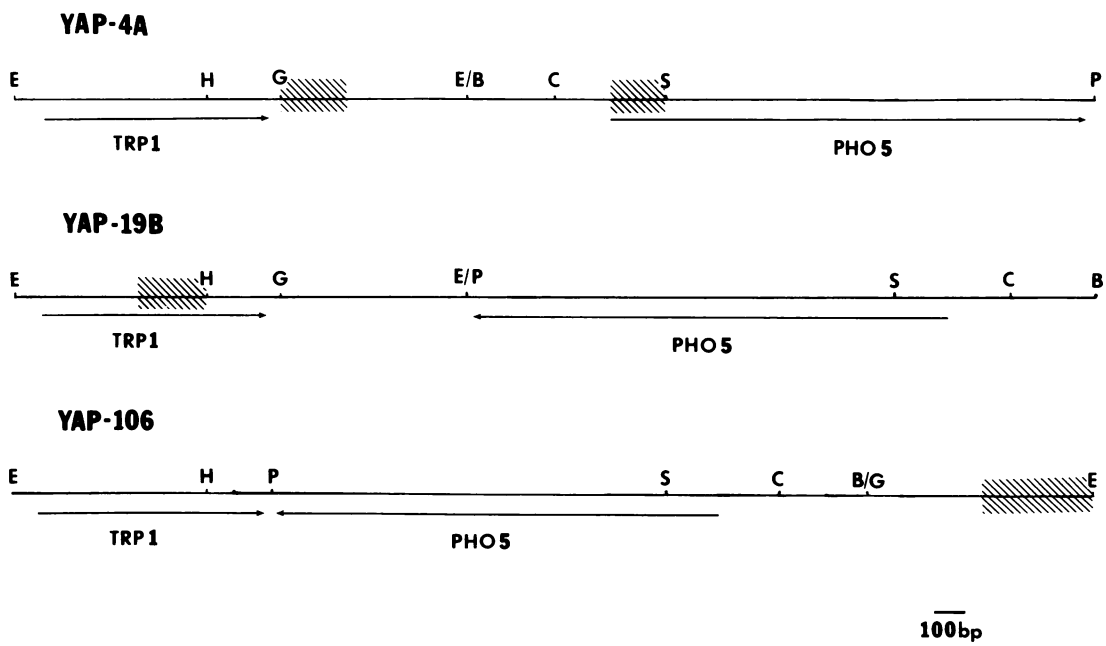

FIG. 1. Schematic representation of the structure of the *PHO5/TRP1/ARS1* plasmids. The shaded regions indicate the gel-purified fragments used as probes in the experiments described in the text. The arrows indicate the direction of transcription and the relative map positions of the *PHO5* and *TRP1* mRNAs. B, *Bam*HI; C, *Cla*I; E, *Eco*RI; G, *Bgl*II; P, *Pst*I; S, *Sal*I.

p-nitrophenyl phosphate in 0.5 ml of 0.1 M sodium acetate buffer (pH 4.2). Reactions were run at 37°C for 10 min and stopped by the addition of 0.12 ml of 25% (wt/vol) trichloroacetic acid and 0.6 ml of saturated sodium carbonate. Cells were removed by centrifugation, and the absorbance was measured at 420 nm. One unit of enzyme activity was taken as that liberating 1 μmol of *p*-nitrophenol per min.

RESULTS

Mapping of micrococcal nuclease cleavage sites on *PHO5* plasmids. The *PHO5/TRP1/ARS1* plasmids and DNA probes utilized in this study are depicted in Fig. 1. Previously, my laboratory had demonstrated that the nucleosomes on plasmid YAP-4A were positioned in a single nonrandom alignment with the presence of an abnormally broad internucleosomal region in the 5′ sequences of the *PHO5* gene (1). To examine whether the precise positioning and spacing of the nucleosomes were structurally or functionally significant, we have determined the positions of the nucleosomes on alternative constructions of the *PHO5/TRP1/ARS1* plasmids. The plasmid-containing fractions were digested with micrococcal nuclease to similar extents as determined by agarose gel electrophoresis and subsequent Southern hybridization analysis (data not shown). In the experiment depicted in Fig. 2, micrococcal nuclease-treated YAP-19B DNA was cleaved with *Hin*dIII and subsequently hybridized with a ^{32}P-labeled *Hin*dIII-*Eco*RV fragment (226 bp) from the *TRP1/ARS1* region, while micrococcal nuclease-treated YAP-4A was cleaved with *Bgl*II and hybridized with the labeled *Bgl*II-*Nae*I fragment (216 bp) from the *TRP1/ARS1* region. Thus the distance from the *Hin*dIII site to the *Bam*HI site of YAP-19B in the 5′-upstream region of *PHO5* is 624 bp, while from the *Bgl*II site to the *Bam*HI site in YAP-4A the distance is 610 bp, a difference of 14 bp. Therefore, if the nucleosomes of the 5′ region of *PHO5* are located in similar positions between the two plasmids, the fragments generated by micrococcal nuclease cleavage within the linker DNA would be on the average 14 bp longer with YAP-19B chromatin (Fig. 2B) than those seen with YAP-4A chromatin (Fig. 2C), as demonstrated in Fig. 2. Also, an abnormally broad linker region is seen in both plasmids. Since the entire DNA sequence of the *PHO5/TRP1/ARS1* plasmid is known, and by analyzing multiple micrococcal nuclease digests of each sample and densitometric tracings of each autoradiograph, I am able to place the nucleosomes (within statistical error) relative to the DNA sequence of the *PHO5* gene as

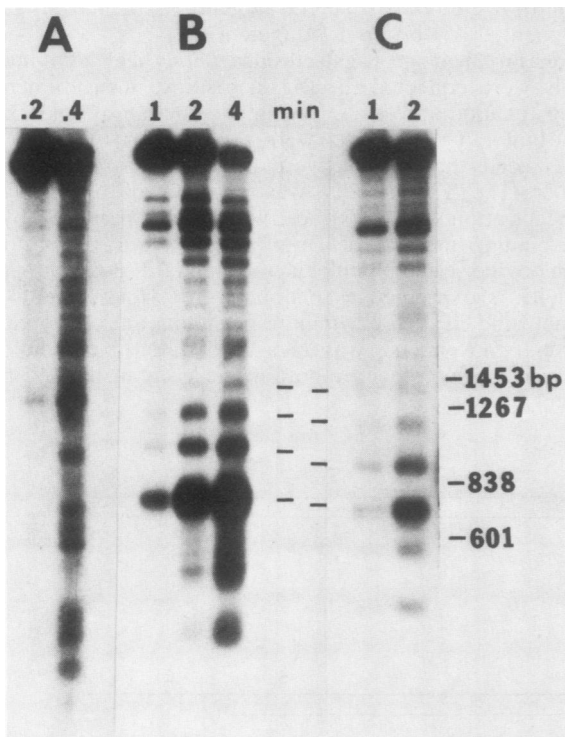

FIG. 2. Nucleosome positioning of the *PHO5* gene. A minichromosome-containing fraction was prepared from various strains grown in high-phosphate media and digested with micrococcal nuclease. The extracted DNA was subsequently digested with the appropriate restriction endonuclease, fractionated on the same 1.2% agarose gel, transferred to nitrocellulose, and probed with the ^{32}P-labeled probes as discussed in the text (see also Fig. 1). The bars represent peaks obtained from densitometric tracings for easier comparison. The nature of the molecular weight marker is discussed in Materials and Methods. (A) Protein-free YAP-19B DNA was digested with micrococcal nuclease, cleaved with *Hin*dIII, and probed with the labeled 226-bp *Hin*dIII-*Eco*RV fragment derived from the *TRP1/ARS1* region. (B) YAP-19B chromatin treated as described in (A). (C) YAP-4A chromatin digested with micrococcal nuclease, cleaved with *Bgl*II, and probed with the labeled 216-bp *Bgl*II-*Nae*I fragment.

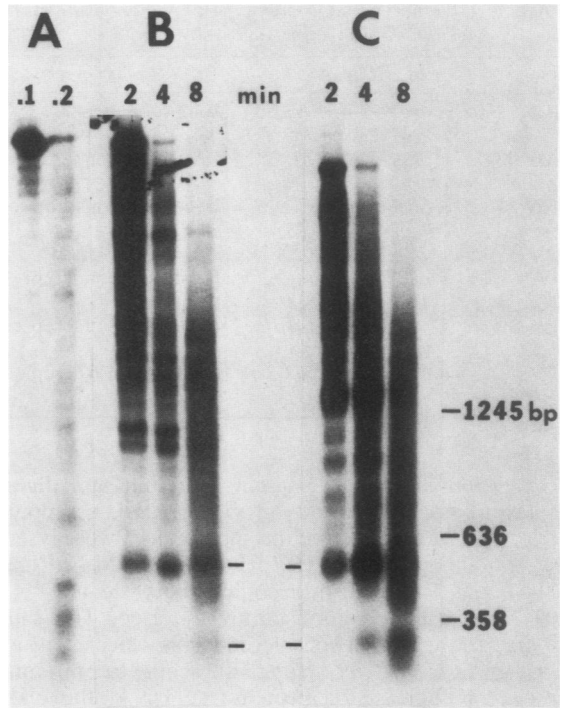

FIG. 3. Effect of upstream sequences on nucleosome positioning of 5′ region of *PHO5* gene. A minichromosome-containing fraction derived from either strain YT1921 or YT19 (see text for description of plasmids) was digested with micrococcal nuclease, and subsequently the extracted DNA was digested with *Sal*I. The DNA was fractionated on the same 1.5% agarose gel, transferred to nitrocellulose, and probed with the labeled 174-bp *Sal*I-*Hae*II fragment derived from the *PHO5* structural sequences. The bars represent peaks obtained from densitometric tracings. The molecular weight standard is derived from purified fragments as follows: 1,254-bp *Sal*I-*Bgl*II fragment, 636-bp *Sal*I-*Bam*HI fragment, and 358-bp *Sal*I-*Cla*I fragment (see Fig. 1). (A) Protein-free YT1921 DNA; (B) YT1921 chromatin; (C) YT19 chromatin.

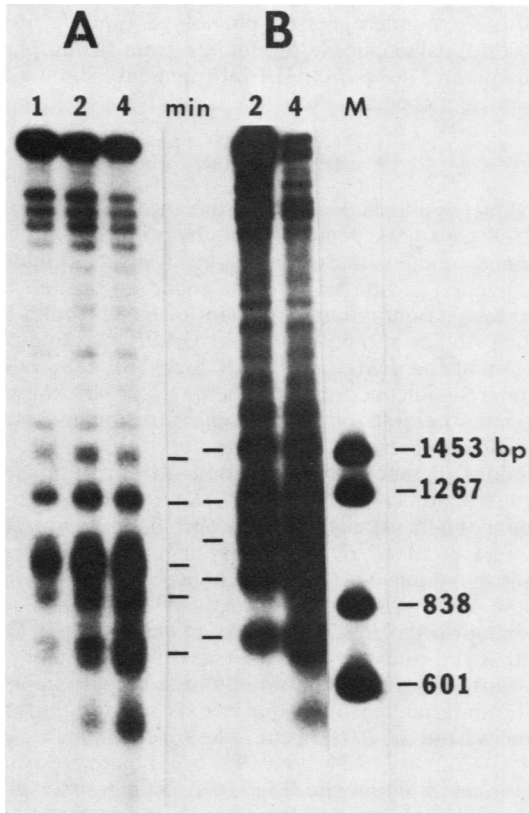

FIG. 4. Nucleosome positioning on the *PHO5* plasmids containing a deletion of the 278-bp *Bam*HI-*Cla*I fragment (see Fig. 1). Experimental details are as described in the legend to Fig. 2. (A) YAP-106-vBC chromatin, digested with *Eco*RI and probed with the labeled 356-bp *Eco*RI-*Rsa*I fragment; (B) YAP-4-vBC chromatin, digested with *Bgl*II and probed with the labeled 216-bp *Bgl*II-*Nae*I fragment. The bars represent peaks obtained from densitometric tracings.

illustrated in Fig. 5. The broad non-nucleosomal region maps to approximately −362 to −424 bp (± 12 bp) upstream from the translational start site (see Fig. 5). Digestion of protein-free YAP-19B DNA with micrococcal nuclease (Fig. 2A) indicates that the cleavage sites seen with the chromatin is not due to the sequence preference of the nuclease. Similar placement of the nucleosomes was determined with YAP-106 chromatin and the same three constructions also containing the *Escherichia coli* plasmid pUC18 (data not shown). These results indicate that the placement of the nucleosomes of the *PHO5* upstream sequences is independent of position or orientation within the plasmids and suggest that a region within the *PHO5* gene itself is responsible for this precise alignment of nucleosomes.

To further rule out any effect by the *TRP1/ARS1* in close proximity, I have constructed a plasmid which contains the 2.1-kb *Eco*RI-*Bam*HI fragment which normally lies upstream of the *PHO5* gene within the genome. Thus the *TRP1/ARS1* sequences are now separated by the 2.1-kb fragment which normally is immediately upstream of the *PHO5* gene, and this inserted region contains no ARS activity itself (L. W. Bergman, unpublished experiment). In this experiment, plasmid (either containing [plasmid YT1921] or lacking [plasmid YT19] the 2.1-kb region) chromatin was digested with micrococcal nuclease, and the purified DNA was cleaved with *Sal*I which cuts within the *PHO5* structural sequences and probed with the labeled *Sal*I-*Hae*II fragment (174 bp) (Fig. 1). This examines the positioning of two nucleosomes upstream of the *Sal*I site (within the *PHO5* gene; see Fig. 1) prior to the region where the sequences diverge (due to the insertion of the 2.1-kb fragment). As indicated by the arrows in Fig. 3, the location of the micrococcal nuclease cleavage sites are identical for pYT19 (Fig. 3C) and pYT1921 (Fig. 3B). Figure 3A is the micrococcal nuclease digestion pattern of protein-free pYT1921. This indicates that the precise position of the nucleosomes is dependent on the *PHO5* sequences (or immediate flanking sequences) and independent of both *TRP1/ARS1* and sequences which normally are located immediately adjacent to the *Bam*HI site in the genome.

To evaluate the sequences responsible for this alignment of nucleosome, plasmids containing a deletion of the 270-bp *Bam*HI-*Cla*I fragment were constructed in the three orientations depicted in Fig. 1. A similar analysis of the micrococcal nuclease digestion patterns was performed with the *Bam*HI-*Cla*I deletion plasmids. For the experiment shown in Fig. 4, micrococcal nuclease-digested YAP-106-ΔBC chromatin was digested with *Eco*RI and subsequently probed with a ^{32}P-labeled *Eco*RI-*Rsa*I fragment (356 bp) from the *TRP1/ARS1* region, while micrococcal nuclease-digested YAP-4A-ΔBC chromatin was digested with *Bgl*II and hybridized with the *Bgl*II-*Nae*I fragment as described previously (Fig. 2C). In this case, the difference from the site of restriction enzyme cleavage to the *PHO5* sequences in the two plasmids is only 4 bp. Thus the micrococcal nuclease cleavage sites should be virtually identical if the nucleosomes are located in the same position in the two plasmids. However, as is seen in Fig. 4A for YAP-106-ΔBC chromatin and Fig. 4B for YAP-4A-ΔBC, the cleavage sites for micrococcal nuclease are different from plasmid to plasmid. However, in each plasmid, the nucleosomes exist in a unique nonrandom orientation. Similar analysis of the cleavage pattern of micrococcal nuclease on YAP-19B-ΔBC chromatin has shown a nonrandom alignment of nucleosomes; however, the nucleosomes are located in positions different from that of either YAP-4A-ΔBC or YAP106-ΔBC chromatin (data not shown). This result suggests that in the case of the plasmids which lack the 270-bp *Bam*HI-*Cla*I fragment, the alignment of the nucleosomes on the *PHO5* gene is now

TABLE 2. Synthesis of β-galactosidase and acid phosphatase in plasmid-transformed strain JL6B grown in low- and high-phosphate media

Plasmid	β-Galactosidase activity[a]		Derepression index[b]	Acid phosphatase activity[c]		Derepression index
	Low P_i	High P_i		Low P_i	High P_i	
pZ270A	1,833.1	11.4	160.8	31.3	1.55	20.2
pZ270B	2,120.4	9.3	228.0	44.1	1.49	29.6
pE602	1,652.7	10.11	162.9	50.1	1.81	27.7
pLG669Z	1,012.1	562.3	1.8	19.0	1.53	12.4
pLG669Z-ΔVXho	7.7	7.0	1.1	19.3	1.65	11.7

[a] β-Galactosidase activity is expressed as nanomoles of *O*-nitrophenyl-β-D-galactoside cleaved per minute per milligram of protein.

[b] Derepression index is defined as the ratio of enzyme activity from cells grown in low-phosphate media to enzyme activity from cells grown in high-phosphate media.

[c] One unit of acid phosphatase activity is expressed as that liberating micromoles of *p*-nitrophenol per minute. The derepression index is defined as the ratio of enzyme units per 1.0 optical density unit at 600 nm of cells grown in low-phosphate media to enzyme units per 1.0 optical density unit at 600 nm of cells grown in high-phosphate media.

TABLE 3. Enzyme levels of cells grown in low- and high-phosphate media

Strain	Plasmid	Low P_i/high P_i	
		β-Galactosidase activity[a]	Acid phosphatase activity[b]
YAT29-40(*pho80*)	pZ270A	1,240.4/1,188.6	14.0/28.7
	pE602	1,326.3/1,262.1	16.3/25.1
YAT42-6B2(*pho4*)	pZ270A	7.8/12.2	1.8/1.9
	pE602	8.1/6.3	1.6/2.0
YAT41-3A(*pho2*)	pZ270A	5.8/10.1	1.9/2.2
	pE602	10.9/8.6	1.5/2.4
YAT242-2A(*pho81*)	pZ270A	5.4/7.2	1.9/1.6
	pE602	10.9/8.6	1.5/2.4
GG100-14D(*pho5*)	pZ270A	1,108.6/10.9	0.6/4.3
	pE602	1,337.3/8.2	0.8/5.1

[a] β-Galactosidase activity is defined as in footnote *a*, Table 2.
[b] Acid phosphatase activity is defined as enzyme units × 10^2 (see footnote *c*, Table 2).

dependent on the position or orientation of the gene within the particular plasmid. This implies also that the "signal" for the precise alignment of the *PHO5* nucleosomes is located in the 270-bp *Bam*HI-*Cla*I fragment.

To evaluate the role of the 270-bp *Bam*HI-*Cla*I fragment, I have utilized a derivative of pLG669Z (6) which lacks the upstream activator sequences of the yeast *CYC1* gene but retains the *CYC1*. TATA region, transcription initiation sites, and the *E. coli lacZ* gene. By using *Xho*I linkers, the 270-bp fragment was inserted into the derivative plasmid in both orientations (pZ270A is the same orientation as in *PHO5*, while pZ270B is the reverse orientation). These plasmids were transformed into yeast strain JL6B, and the production of β-galactosidase and acid phosphatase was measured in response to phosphate level in the growth media. β-Galactosidase is now produced in response to low levels of phosphate in the media in pZ270A- and pZ270B-transformed cells (Table 2), as demonstrated by 200- to 300-fold increase in β-galactosidase in low-phosphate media. This is similar to the levels in cells transformed with pE602, which is a *PHO5-lacZ* protein fusion occurring at amino acid 28 of the acid phosphatase precursor protein. Control experiments with cells containing either pLG669Z or the plasmid lacking the *CYC1* upstream activator sequences pLG669Z-ΔXho show no effect on β-galactosidase activity in response to phosphate level. These results demonstrate that the sequences responsible for the transcriptional regulation of *PHO5* are present on the 278-bp *Bam*HI-*Cla*I fragment. Also, this region, for promoting transcription, is orientation independent as has been seen with other upstream activator sequences (7, 8). The lower derepression index for acid phosphatase production, as compared with that seen for β-galactosidase activity, is due to the production of acid phosphatase in the presence of phosphate by the *PHO3* gene (17). At the present time, however, the difference in acid phosphatase production in strains containing either the *PHO5-CYC1-lacZ* or *PHO5-lacZ* fusions versus strains containing only the *CYC1-lacZ* fusions cannot be explained.

Furthermore, the data in Table 3 demonstrate that the mutant *trans*-acting regulatory alleles for acid phosphatase production confer either high-level constitutive synthesis (*pho80*) or a nonderepressed phenotype (*pho81*, *pho2*, or *pho43*) on β-galactosidase production from fusion plasmids containing the 278-bp *Bam*HI-*Cla*I fragment from the *PHO5* upstream sequences.

DISCUSSION

Previously published studies of the chromatin structure of the *PHO5* gene have demonstrated the presence of precisely positioned nucleosomes along the transcriptionally repressed gene (1). Studies in other eucaryotic gene systems have shown a nonrandom alignment of nucleosomes (5, 12) including studies of the yeast *GAL1-GAL10* promoter region (10, 11) and the HML and HMR loci (16). However, the functional significance of these findings is not known. To investigate the role of nucleosome positioning in *PHO5* repression/derepression and the factors responsible for the nonrandom alignment of nucleosomes, I have utilized various constructions of *PHO5/TRP1/ARS1* plasmids (Fig. 1) to determine the fine structure of the chromatin organization at the 5′ end of the *PHO5* gene. By using the indirect end-labeling technique (24) and DNA probes which originate from the *TRP1/ARS1* region, analysis of the nucleosome positioning on the *PHO5* gene, as revealed in Fig. 2, indicates that the nucleosomes exist in one nonrandom alignment. Furthermore, an abnormally broad (approximately 60 to 70 bp) internucleosomal spacer exists in the 5′-upstream sequences from the *PHO5* gene. The spacer exists at approximately −362 to −424 bp (±12 bp) upstream from the translational initiation site (Fig. 5). A similar analysis of the micrococcal nuclease cleavage sites on the additional *PHO5* constructions has demonstrated that the nucleosomes exist

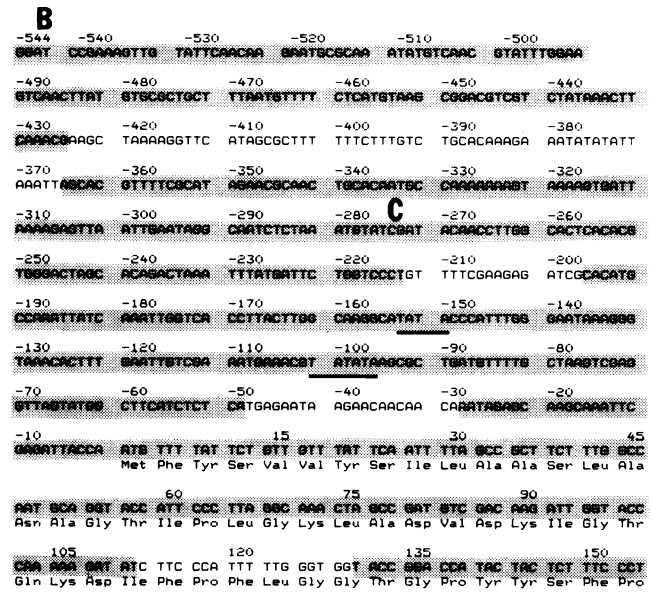

FIG. 5. Schematic representation relating the position of the nucleosomes (indicated by the shaded regions) to the DNA sequence of the 5′ region of the *PHO5* gene. The base pairs are numbered with respect to the *PHO5*-coding sequence. The A residue in the ATG initiation codon represents base pair 1; bases 5′ are numbered consecutively in negative integers, and bases 3′ are numbered consecutively in positive integers. The placement of the nucleosomes was determined as described in the text. The underlined regions are the *PHO5*-TATA-sequences. B, *Bam*HI; C, *Cla*I (see Fig. 1).

in the same position on each plasmid tested (see Fig. 2 for comparison of plasmids YAP-4A and YAP-19B). This result indicates that the positioning of the nucleosomes on the *PHO5* 5′ sequences is independent of the orientation or position of the *PHO5* sequences in the plasmids. This also has been confirmed by using the *PHO5/TRP1/ARS1* constructions cloned into the *E. coli* plasmid pUC18 (6.2 kb in size), suggesting that the nucleosome positioning is not related to the size of the plasmids utilized (data not shown). Furthermore, including the sequences which normally are located upstream of the *PHO5* gene (2.1-kb *Eco*RI-*Bam*HI fragment) has no effect on the location of the nucleosomes at the 5′ end of the *PHO5* gene (Fig. 3). This suggests that the *PHO5* sequences within the 1.9-kb *Bam*HI-*Pst*I fragment are responsible for the unique positioning of the nucleosomes within the *PHO5* 5′-proximal sequences.

To investigate the region of the *PHO5* gene which functions in the nucleosome alignment, I have deleted the 270-bp *Bam*HI-*Cla*I fragment from each of the three plasmids depicted in Fig. 1. A similar analysis of mapping micrococcal nuclease cleavage sites (Fig. 4) has revealed that in each case the location of the cleavage sites is different, suggesting that the location of the nucleosomes is now dependent on either position or orientation of the *PHO5* gene. Thus, this implies that the 270-bp *Bam*HI-*Cla*I fragment, or some part thereof, determines the unique positioning of the nucleosomes.

To assess the functional role of the 270-bp *Bam*HI-*Cla*I fragment, I have utilized a derivative of pLG669Z (termed pLG669Z-ΔXho) which contains the *CYC1* TATA sequences and transcription initiation sites fused to the *E. coli* β-galactosidase gene but lacks a 430-bp *Xho*I fragment which contains the *CYC1* upstream activator sequences (6). After addition of *Xho*I linkers, the *Bam*HI-*Cla*I fragment was cloned into the unique *Xho*I site of pLG669Z-ΔXho in both the correct (termed pZ270A) and opposite (termed pZ270B) orientations. The data in Table 2 demonstrate that the sequences responsible for the transcriptional regulation of *PHO5* (upstream activator sequences of *PHO5*) in response to phosphate level are present on the 270-bp fragment in that β-galactosidase is now synthesized in response to phosphate concentration. Furthermore, the 270-bp fragment contains the sequences which respond to the various *trans*-acting regulatory mutations. The *pho80* mutation confers high-level constitutive synthesis on the *PHO5-CYC1-lacZ* fusion, whereas the *pho2*, *pho4*, and *pho81* mutations impose a nonderepressible phenotype on expression from the fusion plasmid (Table 3). A similar approach has been used to identify the upstream activator sequences of the yeast *GAL10* (7) or *HIS4* (8) gene.

These results, taken together, indicate that the 278-bp *Bam*HI-*Cla*I fragment contains the *PHO5* upstream activator sequences and sequences or structure responsible for a precise positioning of the nucleosomes at the 5′ end of the *PHO5* gene. Interestingly, this fragment is entirely contained in a 353-bp *Sau*3A fragment which is sufficient to mediate a topological change involved in the mechanism of *PHO5* repression/derepression (2). Furthermore, the nucleosome mapping experiments have demonstrated the presence of an abnormally broad internucleosomal spacer within this region (Fig. 2). At the present time, it is not known which of these phenomena are structurally or functionally related; however, the fine-structure/function analysis of a series of DNA deletion mutants constructed in this laboratory within the *Bam*HI-*Cla*I fragment may aid in elucidating the relationships between these observations. Also, these deletion mutants will position the sequences responsible for the transcriptional regulation of *PHO5* gene expression relative to the position of the nucleosomes and spacer DNA. Positioning of the upstream activator sequences within the broad spacer DNA may aid in the ability of the cell to transcriptionally respond to depletion of the phosphate from the culture media.

Recent experiments by Thoma and Simpson have demonstrated that it is possible to construct and introduce into yeast cells a region of DNA that exists as an approximately 70-bp internucleosomal spacer (21). Recent experiments by Lohr investigating the structure of the *GAL1-GAL10* upstream activator region has demonstrated an apparent loss of the normal 10-bp DNase I ladder pattern, suggesting an abnormal chromatin structure within this region (11). Several mechanisms may function in determining the precise nucleosome positioning and the existence of the abnormally broad linker region within the 5′-proximal sequences of the *PHO5* gene. (i) The DNA that is present in the long spacer may have a high degree of secondary structure which precludes formation of a nucleosome in that region. Computer analysis of this region suggests several sequences which could form a stem loop; however, the presence of this structure in vivo is not known. (ii) There is considerable evidence from in vitro chromatin assembly experiments that indicates that there is a sequence preference for nucleosome binding; however, the parameters which determine the specific placement of the nucleosome in these systems are not known (3, 19). It is possible that the regions which surround the broad spacer may have a high affinity for nucleosome binding, thus predicating the existence of the region of non-nucleosomal DNA. In vitro nucleosome assembly experiments that use the 278-bp *Bam*HI-*Cla*I fragment are currently under way to investigate these structural possibilities. (iii) The binding of a regulatory element to this region of the transcriptionally repressed *PHO5* gene may preclude formation of a nucleosome, thus contributing to the precise positioning of the nucleosomes in the surrounding regions. As demonstrated, deletion of the *Bam*HI-*Cla*I fragment from the plasmid constructions has made the placement of the nucleosomes dependent on orientation or position of the sequence within the placement. Recent evidence by Ptashne and co-workers (4) has revealed that the *GAL4* molecule (a positive *trans*-acting regulatory component in the GAL system) may occupy its binding site in the *GAL1-GAL10* promoter in the absence of galactose. Furthermore, using *PHO5-CYC1-lacZ* fusions, I have obtained preliminary evidence for a bound regulatory element associated with the *PHO5 Bam*HI-*Cla*I fragment under repressed growth conditions (L. W. Bergman, D. C. McClinton, S. L. Madden, and L. H. Preis, submitted for publication), but the nature of this element is not known. However, the titration of a negative component by the presence of additional copies of the *PHO5* upstream sequences (present on the *PHO5-CYC1-lacZ* fusion plasmids) may explain the observation of a two- to threefold increase in the derepression index for acid phosphatase production (Table 2).

In summary, I have demonstrated that the precise positioning of the nucleosomes in the 5′ sequences of the *PHO5* gene is determined by the sequences or protein-DNA interactions present on a DNA fragment which also functions in the transcriptional regulation of the *PHO5* gene in response to the phosphate level of the culture media. Continued studies of this region may aid in an understanding of the structure/function relationships between the nucleosome positioning and gene expression and the structural features responsible for nucleosome positioning in this system.

ACKNOWLEDGMENTS

This work was supported by a Public Health Service grant from the National Institute of General Medical Sciences.

I thank Lisa Preis and Barbara Timblin for technical assistance and Audrey Ellis for preparation of the manuscript.

LITERATURE CITED

1. **Bergman, L. W., and R. A. Kramer.** 1983. Modulation of chromatin structure associated with derepression of the acid phosphatase gene of *Saccharomyces cerevisiae*. J. Biol. Chem. **258**:7223–7227.
2. **Bergman, L. W., M. C. Stranathan, and L. H. Preis.** 1986. Structure of the transcriptionally repressed phosphate-repressible acid phosphatase gene (*PHO5*) of *Saccharomyces cerevisiae*. Mol. Cell. Biol. **6**:38–46.
3. **Chao, M. V., J. Gralla, and H. G. Martinson.** 1979. DNA sequence directs placement of histone cores on restriction fragments during nucleosome formation. Biochemistry **18**: 1068–1074.
4. **Giniger, E., S. M. Varnum, and M. Ptashne.** 1985. Specific DNA binding of GAL4, a positive regulatory protein of yeast. Cell **40**:767–774.
5. **Gottesfeld, J. M., and L. S. Blommer.** 1980. Nonrandom alignment of nucleosomes on 5S RNA genes of *Xenopus laevis*. Cell **21**:751–760.
6. **Guarente, L., and M. Ptashne.** 1981. Fusion of *Escherichia coli* LacZ to the Cytochrome C gene of *Saccharomyces cerevisiae*. Proc. Natl. Acad. Sci. USA **78**:2199–2203.
7. **Guarente, L., R. R. Yocum, and P. Gifford.** 1982. A GAL10-CYC1 hybrid yeast promoter identifies the GAL4 regulatory sregion as an upstream site. Proc. Natl. Acad. Sci. USA **79**: 7410–7414.
8. **Hinnebusch, A. G., G. Lucchini, and G. R. Fink.** 1985. A synthetic His4 regulatory element confers general amino acid control on the Cytochrome C gene (CYC1) of yeast. Proc. Natl. Acad. Sci. USA **82**:598–502.
9. **Lemire, J. T., T. Willcocks, H. O. Halvorson, and K. A. Bostian.** 1985. Regulation of repressible acid phosphatase gene transcription in *Saccharomyces cerevisiae*. Mol. Cell. Biol. **5**:2131–2141.
10. **Lohr, D.** 1983. The chromatin structure of an actively expressed, single copy yeast gene. Nucleic Acids Res. **11**: 6755–6773.
11. **Lohr, D.** 1984. Organization of the GAL1-GAL10 intergenic control region chromatin. Nucleic Acids Res. **12**:8457–8474.
12. **Louis, C., P. Schedl, B. Samal, and A. Worcel.** 1980. Chromatin structure of the 5S RNA genes of *Drosophila melanogaster*. Cell **22**:387–392.
13. **Lovett, M., D. G. Guincy, and D. R. Helinski.** 1974. Relation complexes of plasmids ColE1 and ColE2: unique site of the nick in the open circular DNA of the relaxed complexes. Proc. Natl. Acad. Sci. USA **71**:3854–3857.
14. **McGhee, J. D., and G. Felsenfeld.** 1980. Nucleosome structure. Annu. Rev. Biochem. **49**:1115–1156.
15. **Miller, J. H. (ed.).** 1974. Experiments in molecular genetics. Cold Spring Harbor Press, Cold Spring Harbor, N.Y.
16. **Nasmyth, K. A.** 1982. The regulation of yeast mating-type chromatin structure by SIR: an action at a distance affecting both transcription and transposition. Cell **30**:567–578.
17. **Rogers, D. T., J. M. Lemire, and K. A. Bostian.** 1982. Acid phosphatase polypeptides in *Saccharomyces cerevisiae* are encoded by a differentially regulated multigene family. Proc. Natl. Acad. Sci. USA **79**:2157–2161.
18. **Rubin, G. M.** 1974. Three forms of the 5.8S ribosomal RNA species in *Saccharomyces cerevisiae*. Eur. J. Biochem. **41**: 197–202.
19. **Simpson, R. T., and D. W. Stafford.** 1983. Structural features of a phased nucleosome core particle. Proc. Natl. Acad. Sci. USA **80**:51–55.
20. **Southern, E. M.** 1975. Detection of specific sequences among DNA fragments separated by gel electrophoresis. J. Mol. Biol. **98**:503–517.
21. **Thoma, F., and R. T. Simpson.** 1985. Local protein-DNA interactions may determine nucleosome positions on yeast plasmids. Nature (London) **315**:250–252.
22. **Tohe, A., S. Inouye, and Y. Oshima.** 1981. Structure and function of the PHO82-pho4 locus controlling the synthesis of repressible acid phosphatase of *Saccharomyces cerevisiae*. J. Bacteriol. **145**:221–232.
23. **Weisbrod, S.** 1982. Active chromatin. Nature (London) **297**: 289–295.
24. **Wu, C.** 1980. The 5′-ends of *Drosophila* heatshock genes in chromatin are hypersensitive to DNaseI. Nature (London **286**:854–860.
25. **Yanisch-Perron, C., J. Vieira, and J. Messing.** 1985. Improved M13 phage cloning vectors and host strains: nucleotide sequences of the M13mp18 and pUC19 vectors. Gene **33**:103–119.